Optics Communications 283 (2010) 4017–4024

Contents lists available at ScienceDirect

Optics Communications

journal homepage: www.elsevier.com/locate/optcom

The extraordinary optical transmission through double-layer gold slit arrays

Suxia Xie [a,b], Hongjian Li [a,b,*], Shaoli Fu [a], Haiqing Xu [a], Xin Zhou [a,b], Zhimin Liu [a]

[a] College of Physics Science and Technology, Central South University, Changsha 410083, China
[b] College of Materials Science and Engineering, Central South University, Changsha 410083, China

ARTICLE INFO

Article history:
Received 21 November 2009
Received in revised form 6 June 2010
Accepted 7 June 2010

Keywords:
Double-layer gold film
Slit width
Transmission resonances

ABSTRACT

We present the numerical investigation of the optical transmission through a periodic gold nano-slit structure composed with two non-identical layers, and compare it with that of double-layer structure with two identical layers. The optical enhancement is attributed to the surface Plasmon resonance collaborated with the localized waveguide resonance. It is shown that the transmission behaviors are strongly dependent on the layer separation and lateral displacement between the two single metallic gratings. Especially, it is found that extraordinary transmission exists even if the slit of one layer shifts laterally over that of the other one to the situation that no light can propagate directly when layer separation $D=0$. When the slit widths of two layers are not equal, the surface plasmon resonance peak alternately decreases and increases twice, and the localized waveguide resonance peak appears at a longer wavelength as the lateral displacement varies for a non-zero layer separation, which differs from the situation with two identical layers. These transmission properties of the structures show promise for applications in optical devices.

1. Introduction

The enhanced optical transmission through metal films with periodic sub-wavelength holes was found firstly by Ebbesen in 1998 [1], which has aroused a considerable interest due to its possible numerous applications in optics such as frequency selection and photolithography [2–5], and so on. It is found that the enhanced optical transmission through periodic metal hole arrays originates from the resonance of surface Plasmon mode, which is a surface wave generated by the interaction between the surface charge oscillation and the electromagnetic field of the light. The enhancement also depends on the array geometry (diameter, periodicity, and thickness of the metal film), light wavelength, angle of incidence, as well as material of a film [6–10]. For periodic slit arrays, Porto et al. [11], who base their arguments on the transfer matrix formalism claim that surface plasmon excitation enhances the efficiency. However, Treacy [12] uses a rigorous dynamical diffraction model to compute the transmission of light through slit arrays in metallic films, and he does not attribute any specific role to surface plasmon excitations, emphasizing the cooperation between evanescent and guided modes in determining the overall transmission efficiency of the slit array. Enhanced optical transmission studies have been focused traditionally on single-layer structures [13]. It is until quite recently when studies of multilayer hole and slit arrays have gained more attention. Transmission through double-layer smooth surfaces [14,15], hole and slit arrays [15–18] with different shapes and dimensions has been investigated. These systems are always consisted of two identical single layers; however, double-layer structures with slit width of one layer different from that of the other layer are seldom investigated.

In this paper we present a double-layer structure composed of two non-identical single layers with periodic nano-slits, and simulations for structure with two identical layers are included as base lines to compare the results to. In the structure with non-identical single layers, slit width of one layer is different from that of the other one. Transmissions of the double-layer metal slit arrays for both situations are investigated as the layer separation and lateral displacement vary. The underlying transmission mechanisms are attributed to the collaboration of the surface plasmon resonance and the localized waveguide resonance. Transmission peaks of both resonances behave differently along with lateral displacement varying for different layer separations, and the related electric field distributions simulated at the resonance wavelengths are helpful to understand the physical mechanism.

2. Theory

The propagation of the light in the metal is described by the Maxwell equations which are coupled with the oscillations of quasifree electrons in the metal as follows:

$$\nabla \times \vec{E} = -\mu_0 \frac{\partial \vec{H}}{\partial t}, \quad (1)$$

$$\nabla \times \vec{H} = \varepsilon_0 \frac{\partial \vec{E}}{\partial t} + \vec{J}, \quad (2)$$

* Corresponding author. College of Physics Science and Technology, Central South University, Changsha 410083, China. Tel.: +86 731 88830863; fax: +86 731 88877805.
E-mail address: lihj398@yahoo.com.cn (H. Li).

0030-4018/$ – see front matter © 2010 Elsevier B.V. All rights reserved.
doi:10.1016/j.optcom.2010.06.031

$$\frac{\partial \vec{J}}{\partial t} + \gamma \vec{J} = \varepsilon_0 \omega_p^2 \vec{E} \ . \tag{3}$$

where $\vec{E}$ and $\vec{H}$ are the electric and magnetic field vectors, respectively. $\vec{J}$ is the current density (A/cm^2) and equal to the time derivative of the metal polarization, i.e. $\vec{J} = \partial \vec{P} / \partial t$, ε_0 and μ_0 are the permittivity and magnetic permeability of the vacuum, respectively.

Calculations are performed using the finite-difference time-domain (FDTD) method [19,20], which solves Maxwell's equations by discretizing both time and space and by replacing derivatives with finite differences. The structures are irradiated normally by a TM-polarized plane wave pulse ($\vec{E}y$, $\vec{E}z$, $\vec{H}x \neq 0$). The spectrum width of this pulse can cover the range desired in the calculation. The temporal response of the structure is saved after calculation. Through a simple Fourier transform, the transmission spectra of the structure can be obtained.

The dielectric constant of Au metallic grating is described by the Drude model [21]:

$$\varepsilon_m(\omega) = 1 - \frac{\omega_p^2}{\omega^2 + i\gamma\omega} , \tag{4}$$

where ω_p is the plasma frequency and γ is the collision frequency, related to energy loss. The parameters used in the Drude model for Au are $\omega_p = 1.374 \times 10^{16}\ \mathrm{s}^{-1}$ and $\gamma = 4.08 \times 10^{13}\ \mathrm{s}^{-1}$, taken from Ref. [22].

It is well known that at the metal-dielectric interface, the surface plasmon mode obeys the following dispersion relation:

$$k_{sp} = k_0 \sqrt{\frac{\varepsilon_d \varepsilon_m}{\varepsilon_d + \varepsilon_m}} \tag{5}$$

where k_0 is the wave vector of the incident light and ε_m and ε_d are the permittivities of the metal and the dielectric, respectively. And in a metal film with periodic slit array, the interaction between light and the surface plasmon polariton obeys momentum and energy conservation given by [1]:

$$|\vec{k}_{spp}| = |\vec{k}_0 \sin\phi + j\vec{G}_y| \tag{6}$$

where $|\vec{k}_{spp}|$ is the wave vector of the surface plasmon polariton, $\vec{k}_0 \sin\phi$ is the in-plane component of the incident wave vector, $\vec{G}_y$ is the reciprocal lattice vector which for a slit array has the value $|\vec{G}_y| = 2\pi / p$, p is the lattice periodicity and j is integer. This equation can be used to analytically predict the approximate excitation frequencies at which the incoming light couples to the surface plasmon polaritons on a double layer slit array via grating coupling.

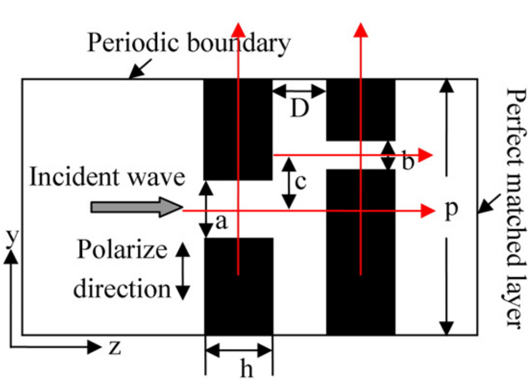

Fig. 1. *yz* cross section of the computational domain consisting of a single unit cell of the double-layer slit arrays. A normal incident light wave polarized along *y* direction illuminates the arrays along *z* direction. Periodic boundary conditions are imposed on the surfaces perpendicular to the gold films, while perfect matched layers are imposed at the left and right surfaces.

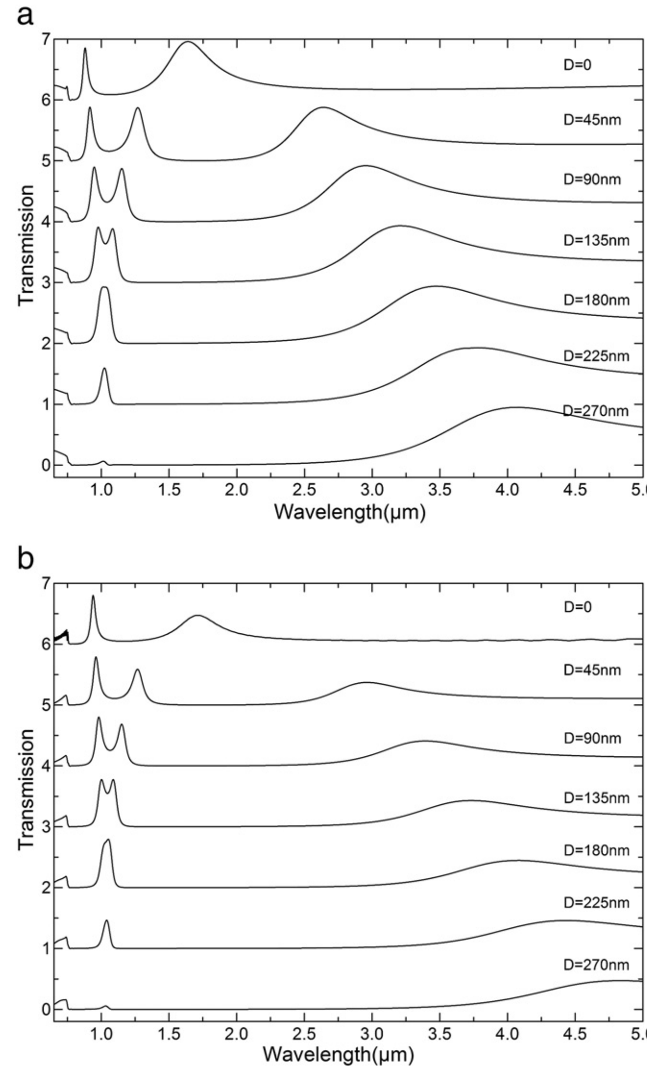

Fig. 2. Normalized transmission through the double-layer metal slit arrays for different layer separations ranging from 0 to 270 nm in step of 45 nm for the structure with two identical layers ($a = b = 150$ nm) shown in (a) and with two non-identical layers ($a = 150$ nm, $b = 50$ nm) shown in (b).

3. Results and discussion

Many researchers show that the enhanced transmission is attributed to the surface plasmon resonance arising from the surface periodicity [11,23], and should be independent of hole shape. Klein et al. [24] demonstrated experimentally that there is strong influence of hole shape on the enhanced transmission. Recently Z.C. Ruan and M. Qiu [25] investigated the property of the resonance by analyzing the electromagnetic band structures in the structured metal film. They showed that the enhanced transmission through metallic film with a periodic array of sub-wavelength holes results from two different resonances: (i) localized waveguide resonances where each air hole can be considered as a section of metallic waveguide with both ends open to free space, forming a low-quality-factor resonator, and (ii) well-recognized surface plasmon resonances due to the periodicity. In addition, we proved previously that, for the double-layer structure with two identical single layers, there are two such resonances, and as the periodicity increases the surface plasmon resonance peak varies obviously, but the localized waveguide resonance is nearly independent on it [16]. The transmission spectrum of the periodic metal slit array behaves similarly to that of the periodic hole array. For a periodic metal slit array, the two extraordinary transmission peaks

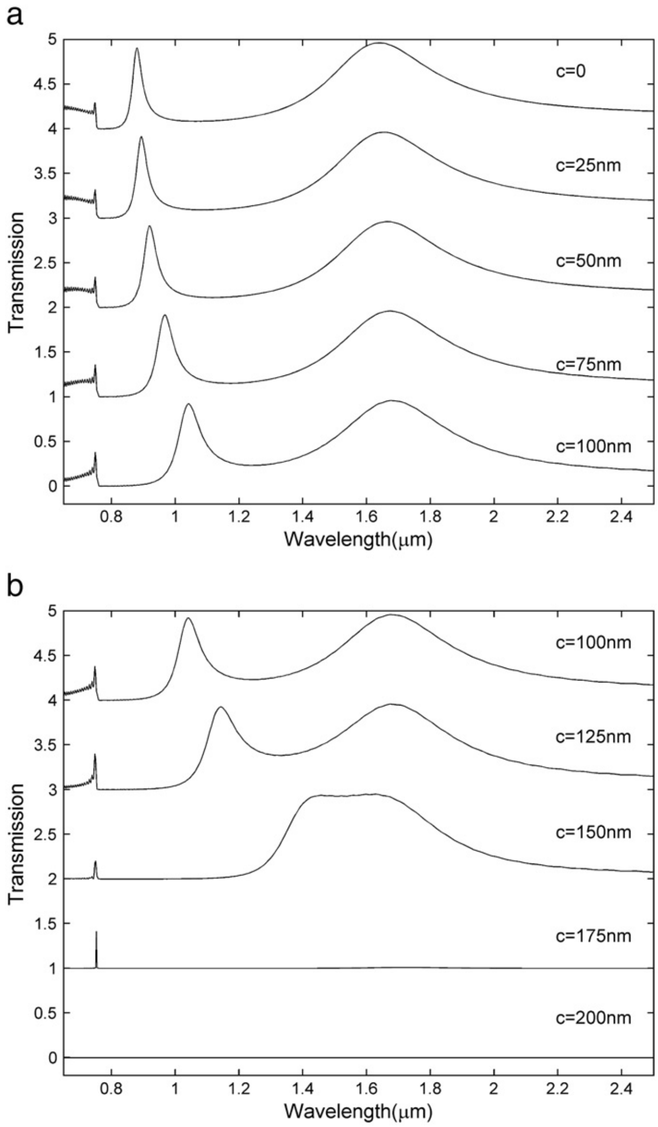

Fig. 3. Transmission spectra for lateral displacement varying from $c = 0$ to $c = 200$ nm in step of 25 nm of the double-layer structure with two identical layers $a = b = 150$ nm and layer separation $D = 0$.

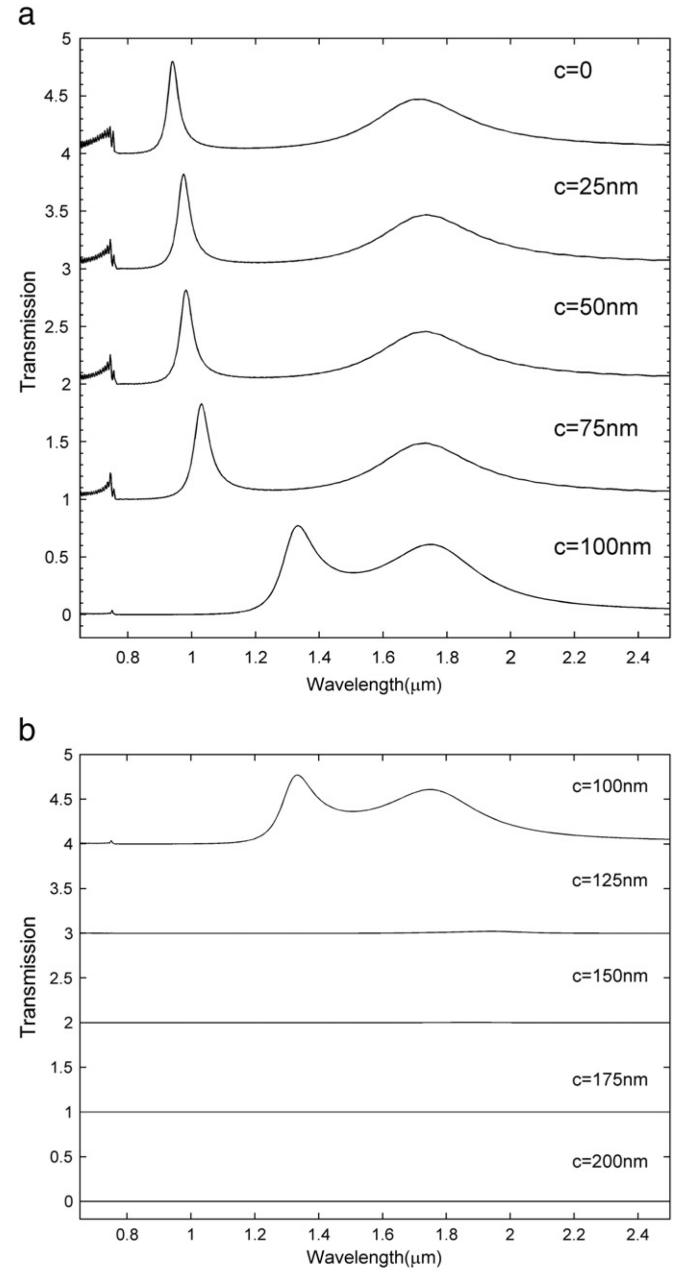

Fig. 4. Transmission spectra for lateral displacement varying from $c = 0$ to $c = 200$ nm in step of 25 nm of the double-layer structure with slit width $a = 150$ nm of the first layer, $b = 50$ nm of the second layer, and layer separation $D = 0$.

can also be attributed to the surface plasmon resonance and the localized waveguide resonace. In this paper, we study double-layer structure composed of two non-identical layers of gold slit arrays basing on structure with two identical layers. And both resonance modes are modified by the coupling between the layers.

As depicted in Fig. 1 the structure lies on the *yz* plane and consists of two single layers of gold nano-slit arrays. Dielectric medium filling in the slits and surrounding the structure is air. The incoming wave is considered to be normal to the structure with the $\vec{E}$ field polarized along the y axis. The thickness of each layer $h = 300$ nm, the lattice parameter $p = 750$ nm are kept constant in all the simulations. The slit widths of the two layers are noted as a and b, respectively. c is the lateral displacement, which is the distance of the slit center of the first layer to that of the second layer in y direction, and D is the layer separation. Transmission spectra and electric fields inside and near the metal films are simulated using the FDTD method. Periodic boundary conditions are imposed on the top and bottom boundary surfaces perpendicular to the gold film, while at the left and right surfaces of the lattice, it is attached by the perfect matched layers (PML), which associate with an approach involving a medium that in theory absorbs electromagnetic waves without any reflection at all frequencies and angles of incidence proposed by Berenger in 1994 [26].

We now study the transmission properties when the two gold slit arrays are set coaxially, first for the situation of two identical slit arrays as shown in Fig. 2(a), and then for the situation of two arrays with different slit widths as shown in Fig. 2(b). For both situations, it can be obtained that, when $D = 0$, the double-layer structure is equivalent to a single layer film with a twice thickness, there are two extraordinary transmission resonances. According to the peak positions, the shorter wavelength transmission peak is considered to be the surface plasmon resonance induced by the periodicity, and the longer wavelength resonance peak is associated with the localized waveguide resonance related to the slit shape and size. At the rear surface of the first layer and the front surface of the second layer of the structure, the surface plasmon modes can be supported, respectively. When the two single layers of gold slit array are put close to each

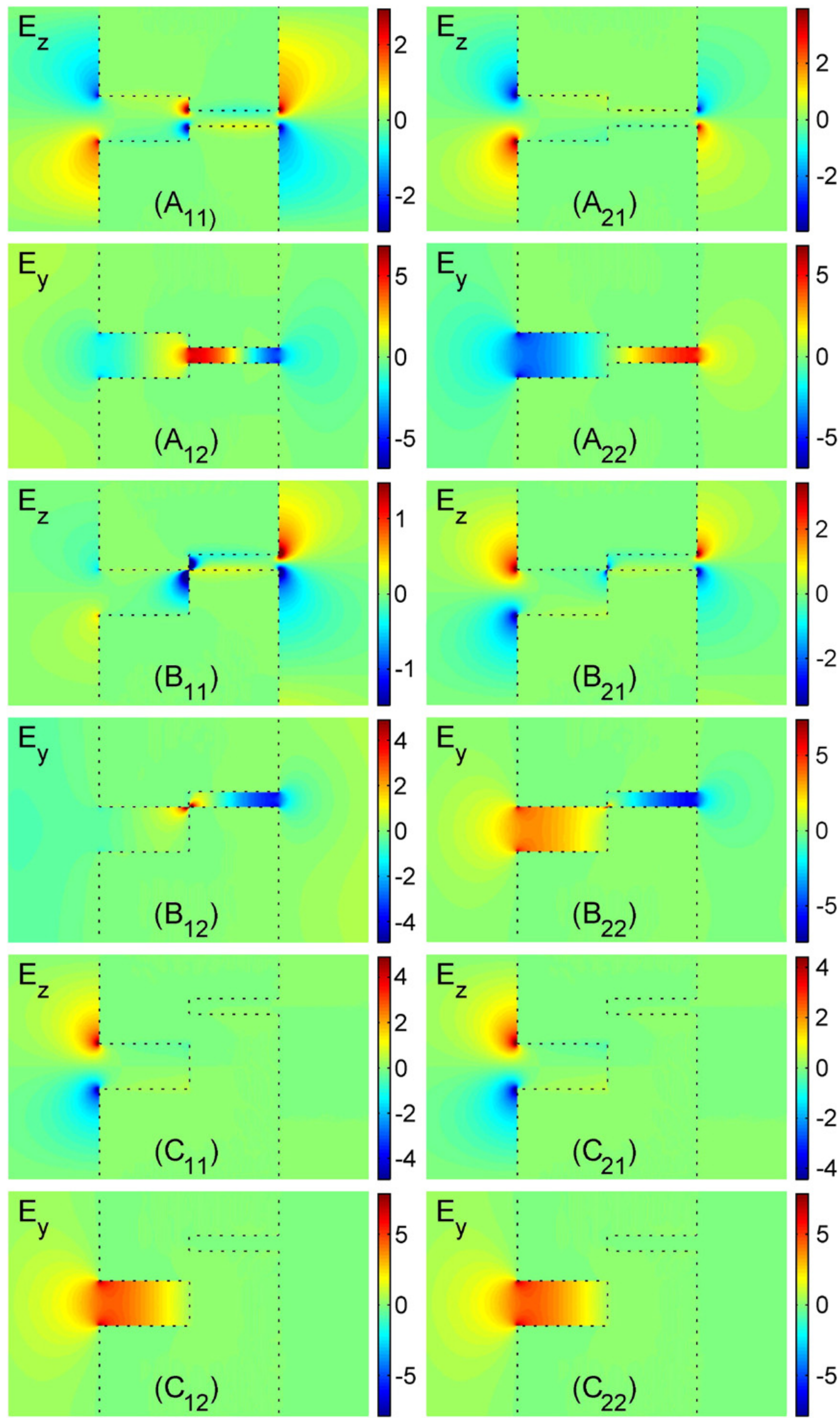

Fig. 5. The field distributions on the *yz*-plane of *Ez* and *Ey* (A_{11}–A_{12}) at the surface plasmon resonance wavelength $\lambda = 0.9410$ μm, and (A_{21}–A_{22}) at the localized waveguide resonance wavelength $\lambda = 1.7198$ μm, for $c = 0$; *Ez* and *Ey* (B_{11}–B_{12}) at the surface plasmon resonance wavelength $\lambda = 1.3336$ μm, and (B_{21}–B_{22}) at the localized waveguide resonance wavelength $\lambda = 1.7439$ μm, for $c = 100$ nm; and *Ez* and *Ey* (C_{11}–C_{12}) at the surface plasmon resonance wavelength $\lambda = 1.3336$ μm, and (C_{21}–C_{22}) at the localized waveguide resonance wavelength $\lambda = 1.7439$ μm, for $c = 200$ nm with layer separation $D = 0$.

other, the two surface plasmon modes will couple to form a coupled surface plasmon mode, which can propagating along the air gap, and the electromagnetic radiation from the first layer can tunnel into the second layer through the gap. The smaller the layer separation is, the stronger the coupling of the surface plasmon from the two layers is (except the $D = 0$ situation). The strong coupling effect results in the splitting of the surface plasmon resonance peak. In addition, the two peaks exhibit the redshifts and blueshifts, respectively. When D is increased to about 190 nm, the two peaks degenerate into a single transmission peak. The wavelength of this single transmission peak hardly changes when D further increases, while the transmittance monotonously decreases, because the two single layers have almost decoupled. Meanwhile, with the layer separation increasing, the localized waveguide redshifts noticeably, and the possible reason for the redshift of the localized waveguide mode is due to surface modes coupling between the two layers similar to the mechanism of the transmission peak redshift with the slit width increasing of a single layer structure [27]. In addition, the center wavelength of the localized waveguide resonance for structure with non-identical layers is obviously larger than that for the structure with identical layers. In order to investigate and analyze conveniently, we choose the situation $D=0$ and $D=195$ nm where the surface plasmon resonance has only one resonance peak.

Transmissions are calculated for the structure with both situations composed of identical layers ($a=b=150$ nm) and non-identical layers ($a=150$ nm, $b=50$ nm)) with $D=0$. From Figs. 3 and 4, it can be seen that, for the case $D=0$, as lateral displacement c increases, transmissions share the same trend for both structures with identical layers and non-identical layers. It is obtained that the surface plasmon resonance peak redshifts gradually with peak magnitude varying little along with slit center of the second layer moving up from $c=0$ to $c=200$ nm, while for the localized waveguide resonance peak, there is almost no change of either the center peak wavelength or the peak shape. These phenomena mentioned above for both types of resonances may be related to the cavity resonance mode excited and coupling in the stepped slit. For structure with identical films, when c increases further to 150 nm, the surface plasnmon resonance peak and the localized waveguide resonance peak merge with each other (as shown in Fig. 3(b)). For the structure with two non-identical layers, the merging appears at about $c=100$ nm (as shown in Fig. 4(a)). $c=150$ nm for the structure with identical layers and $c=100$ nm for the structure with non-identical layers are situations that the top edge of the slit of the first layer is aligned to the bottom edge of the slit of the second layer. When slit center of the second layer moves upwards additionally, both the surface plasmon resonance and the localized waveguide resonance peaks decrease sharply to almost no optical transmission (as shown in Fig. 3(b) and 4(b)), in addition, it is found that the surface plasmon resonance peak decreases much more sharply than that of the localized waveguide resonance one. Which may be associated with that the excited surface plasmon on the left surface of the first layer and that on the right surface of the second layer couples weakly as a result of the absorption inside the thick metal.

Fig. 5 shows distributions of the electric field at the surface plasmon resonance and localized waveguide resonance wavelengths of the structure composed of layers with different slit widths ($a=150$ nm, $b=50$ nm) when the lateral displacement are $c=0$ (A_{11}–A_{22}), $c=100$ nm (B_{11}–B_{22}), and $c=200$ nm (C_{11}–C_{22}), respectively, with $D=0$. The system equals to a thicker single layer grating with slits of inconsistent width. From Fig. 5(A_{11}–A_{12}), it is shown that for the surface plasmon resonance of the structure with $c=0$, Ez distributes at edges of the inconsistent slit, giving rise to accumulated charges at the sharp corners, where these oscillating charges on opposite edges of the slit behave as electric dipoles. These dipoles are flanged by opposite surface charges and these periodic charges establish a standing wave resonance in the slit. The local charge dipole oscillation can also be revealed from Ey that is mostly concentrated at both ends of slit of each layer. Ey at the joint of the two metal layers has the same electric sign, and it is strengthened inside the inconstant slit. For the localized waveguide resonance of the structure with $c=0$, electric field distributions are shown in Fig. 5(A_{21}–A_{22}). It can be seen that besides the opposite symmetry property of the field modes, nearly no Ez field enhancement is noticed at edges and the exit of the inconsistent slit as shown in Fig. 5(A_{21}), whereas it is strong for the surface plasmon resonance as shown in Fig. 5(A_{11}). It is known that for each layer, each slit can be considered as a waveguide with both ends open to the air. When the two layers of slit arrays with different slit widths are put coaxially with layer separation $D=0$, the slit is similar to a longer inconsistent waveguide. There is a wave node of Ey in the wide slit and the narrow one along the z-direction respectively, which can be expressed by the Febry–Perot effect [26,28,29]. Interestingly, if the slit of one layer shifts laterally over that of the other one to the situation that no light can propagate directly with zero layer separation enhanced field distributions can still be obtained (as shown in Fig. 5(B_{11}–B_{22})). Fields Ez and Ey at the surface plasmon resonance wavelength are still strong and localized mostly at the edges and both ends of the slit of the second layer, respectively, corresponding to the high transmission peak as shown in the Fig. 4 ($c=100$ nm). At the localized waveguide resonance wavelength, fields Ez and Ey (as shown in Fig. 5(B_{21}–B_{22})) distribute at locations similar to that for $c=0$, which accords well to the localized waveguide resonance peak trend along with the slit center c of the second layer

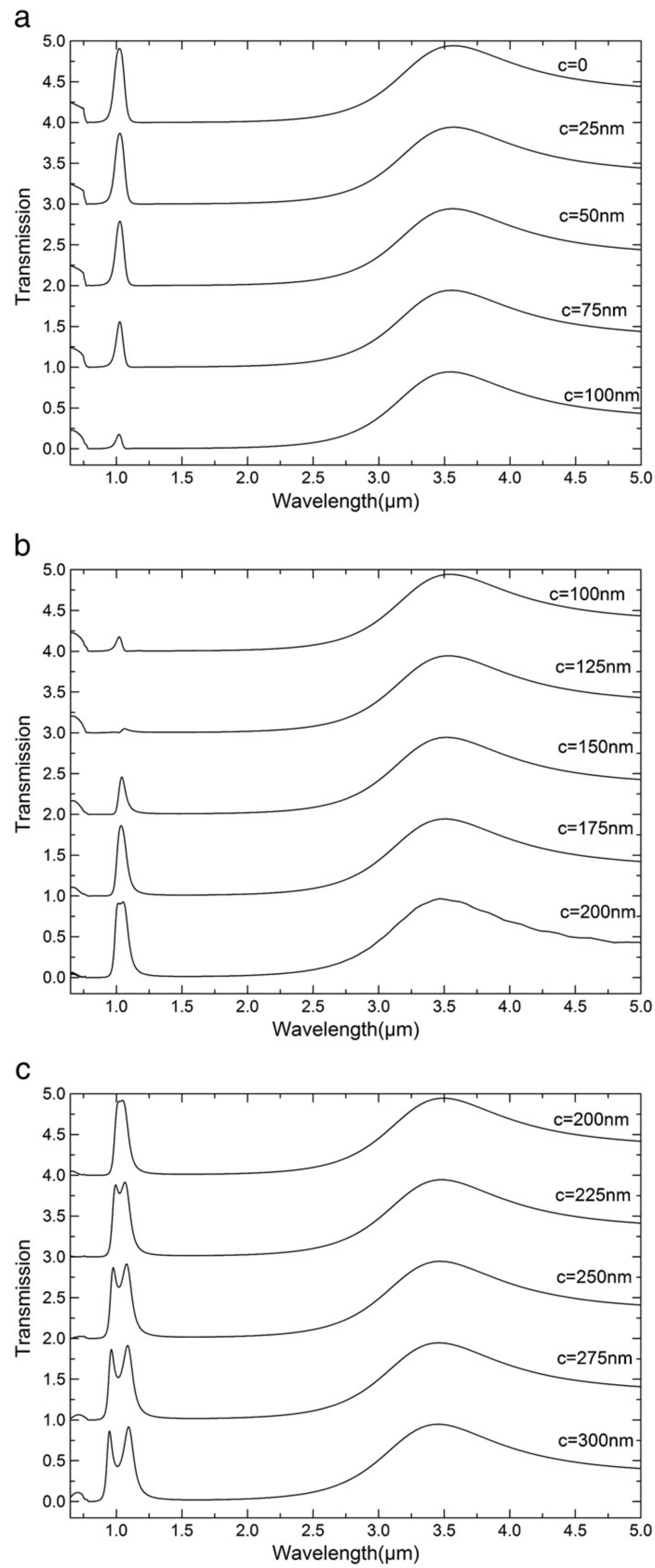

Fig. 6. Transmission spectra for lateral displacement varying from $c=0$ to $c=300$ nm in step of 25 nm of the double-layer structure with two identical layers $a=b=150$ nm and layer separation $D=195$ nm.

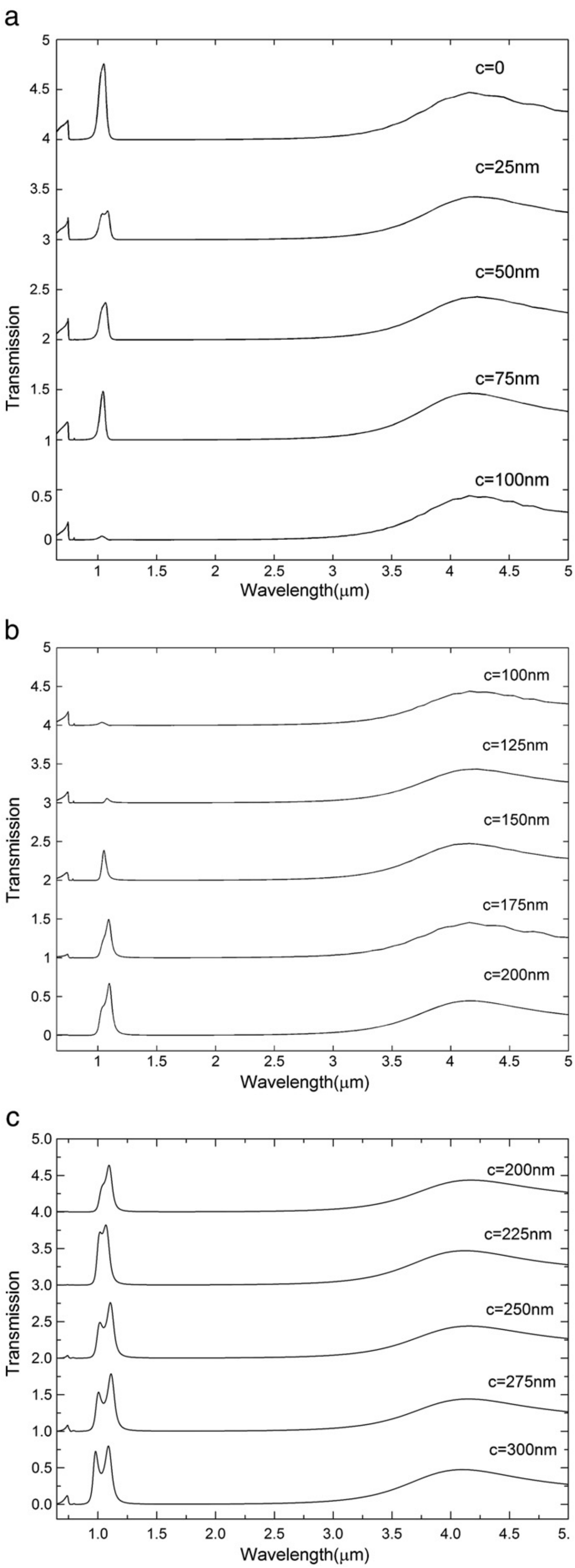

Fig. 7. Transmission spectra for lateral displacement varying from $c=0$ to $c=300$ nm in step of 25 nm of the double-layer structure with $a=150$ nm, $b=50$ nm, and layer separation $D=195$ nm.

moving as shown in Fig. 4. If the slit of the second layer shifts on to $c=200$ nm, there are electric dipoles at the edges of the slit of the first layer (as shown in Fig. 5(C_{11} and C_{21})) and standing waves inside this slit (as shown in Fig. 5(C_{12} and C_{22})), however, there is no electric field distributions absolutely at the exit of the slit in the second layer. It means there is no transmission for the double-layer structure with layer separation $D=0$, which accords well to the transmission spectrum for $c=200$ nm in Fig. 4(b).

Next, we investigate the transmission of the double-layer structure with periodic slit arrays at the layer separation $D=195$ nm, there is exactly only one degenerated transmission for the surface plasmon resonance. In this structure the center of the first layer is fixed at $(y,z)=(0,-(D/2+h/2))$, and slit center of the second layer in the lattice is $(y,z)=(c, (D/2+h/2))$.

Fig. 6(a) and 6(b) show the transmission spectra of the double-layer structure composed of two identical layers ($a=b=150$ nm) with various lateral displacements, and the layer separation is fixed at $D=195$ nm. It is shown when c is increased from 0 to 150 nm, the transmittance of the surface plasmon resonance reduces sharply from 91.0% to 4.2%. If the slit of the second layer shift upwards further, peak value of this resonance increases inversely. When the slit center of the second layer shifts to $c=200$ nm, the transmittance rises back to 90%. When c is larger than 200 nm, such a single transmission peak splits into two separate peaks, and the separation becomes greater as c increases (as shown in Fig. 6(c)) which accords to the results of ref. [18] well. The surface plasmon resonance peak is modulated by the lateral displacement obviously; however, the localized waveguide resonance peak is nearly independent on it. In addition, there is almost no shift for center wavelengths of both types of resonances as the lateral displacement increases.

Here we calculate the transmission spectra of the structure with two non-identical layers at different lateral displacements from 0 to 300 nm. Slit width of the first layer is $a=150$ nm and that of the second layer is $b=50$ nm. It is shown as Fig. 7(a) and (b) that with slit center of the second layer moving up gradually, the surface plasmon resonance peak decreases twice and increases twice. When $c=100$ nm, in other words, bottom edge of the second layer aligned to top edge of the first layer, it is clearly shown that the surface plasmon resonance peak nearly disappears. Additionally, peak value of the surface plasmon resonance increases continuously as c increases further at a range $c>100$ nm. While the localized waveguide resonance peak changes and moves insignificantly in the whole process of c variation. When c is larger than 200 nm, the surface plasmon resonance peak splits into two separate peaks, and the separation becomes greater as c increases (as shown in Fig. 7(c)). In addition, compared Fig. 7(a–c) with Fig. 6(a–c), with layer separation $D=195$ nm, it can be found that surface plasmon resonance peak nearly shares the same center wavelength for both conditions for which is mostly dependent on the periodicity and influenced insignificantly by the slit width; however, center peak wavelength of the localized waveguide resonance is longer for the structure with non-identical layers than that with identical layers. As we know the localized waveguide resonance is associated with the size and shape of the waveguide, so when the slit width is varied, the resonance wavelength will be change dependently.

Simulated results of electric field distributions at resonance wavelengths for layer separation $D=195$ nm are presented. Fig. 8 (A_{11}–A_{12}) show Ez and Ey distributions at the surface plasmon resonance wavelength $\lambda=1.0478$ μm, and Fig. 8(A_{21}–A_{22}) show Ez and Ey distributions at the localized waveguide resonance wavelength $\lambda=4.1562$ μm, respectively, for the double-layer structure with lateral displacement $c=0$. It can be seen that the opposite symmetry

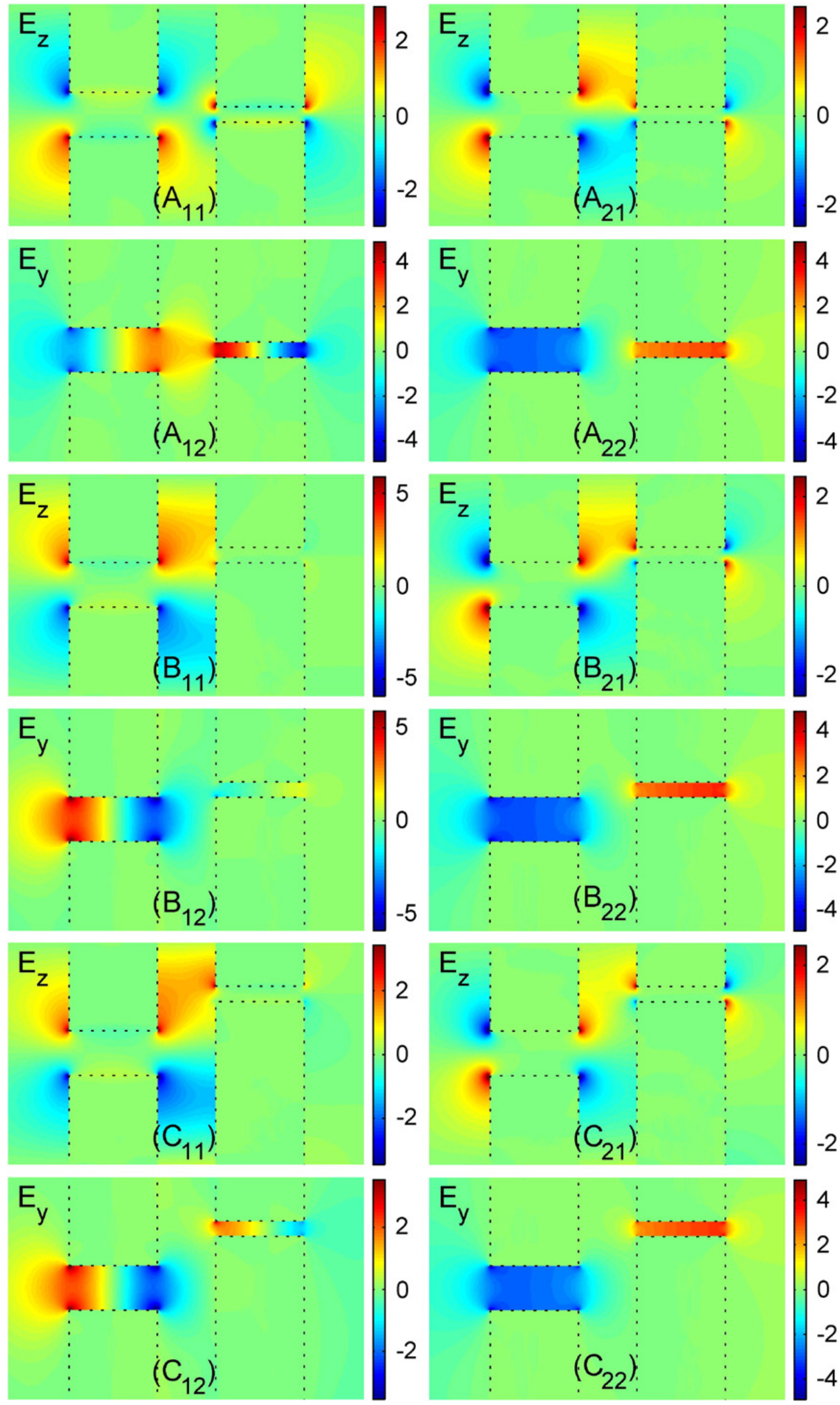

Fig. 8. The field distributions on the *yz*-plane of *Ez* and *Ey* (A_{11}–A_{12}) at the surface plasmon resonance wavelength $\lambda = 1.0478$ μm, and (A_{21}–A_{22}) at the localized waveguide resonance wavelength $\lambda = 4.1562$ μm, for $c = 0$; *Ez* and *Ey* (B_{11}–B_{12}) at the surface plasmon resonance wavelength $\lambda = 1.0348$ μm, and (B_{21}–B_{22}) at the localized waveguide resonance wavelength $\lambda = 4.1562$ μm,, for $c = 100$ nm; and *Ez* and *Ey* (C_{11}–C_{12}) at the surface plasmon resonance wavelength $\lambda = 1.0348$ μm, and (C_{21}–C_{22}) at the localized waveguide resonance wavelength $\lambda = 4.1562$ μm,, for $c = 200$ nm, respectively, with layer separation $D = 195$ nm.

properties of the field modes which coincides with their transmission phases for the different resonances: inside the air gap between the two layers, *Ez* is decoupled for the surface plasmon resonance, however it is intensified for the localized waveguide resonance (as shown in Fig. 8 (A_{11}) and (A_{21})). It is noted there are two nodes inside the slit as shown in Fig. 8(A_{12}), which means that *Ey* field is enhanced at both ends of the slit for each layer. Moreover, electric fields of *Ey* at the exit of the first layer and that at the entrance of the second layer have a uniform electric sign, so it is strengthened inside the air gap for the surface plasmon resonance. However, *Ey* is concentrated in the middle of the slit as a wave node shown in Fig. 8(A_{22}) for the localized waveguide resonance. For the double-layer structure with $c = 100$ nm, *Ez* and *Ey* distributions for the surface plasmon resonance for the first layer are similar to that of the coaxial structure, however, electric intensities are very faint for the second layer as shown in Fig. 8(B_{11}–B_{12}) simulated at surface plasmon resonance wavelength $\lambda = 1.0348$ μm, which leads to a tiny transmission resonance peak in Fig. 7($c = 100$ nm). If the slit of the second layer shifts on to $c = 200$ nm, there are electric dipoles at the edges of the slit of both layers (as shown in Fig. 8(C_{11})), and they constructively couple with each other inside the air gap. *Ey* is distributed at both ends of slit of each layer, and is obviously strengthened in the slit of the second layer (as shown in Fig. 8(C_{12})), which is co-insistent with the increase of the surface plasmon resonance peak in Fig. 7(b) for $c = 200$ nm. For the localized waveguide resonance, electric fields *Ey* and *Ez* show similar distributions for $c = 0$, $c = 100$ nm and $c = 200$ nm for the two layers (as shown in Fig. 8(A_{21}–A_{22}), (B_{21}–B_{22}) and (C_{21}–C_{22})). It corresponds to the invariableness of the localized waveguide resonance peak in Fig. 7.

4. Conclusions

In conclusion, the optical transmission properties of the double-layer metallic periodic nano-slit arrays composed of two identical and non-identical layers are studied by using FDTD method. Transmission spectra and electric field distributions are calculated. It is found that transmissions are influenced dramatically by layer separation and lateral displacement for the two layers of the structures. The enhanced transmissions are attributed to the surface plasmon resonance and the localized waveguide resonance. Split, shift, decrease and increase of the resonance peaks are discovered as the layer separation and lateral displacement vary. It is found there are high transmission peaks though no light can propagate directly for slits of one layer beyond exactly that of the other layer with none separation between layers. When the slit width symmetry of the two layers is broken, there are some modifications of the transmission behavior. The results obtained here may prove a useful guide to design metallic slit optical devices.

Acknowledgments

This work was funded by the excellent doctorate dissertation foundation of Central South University under Grant No. 2008yb039, and the Postgraduate Innovative Project of Hunan Province under Grant No. CX2009B029.

References

[1] T.W. Ebbesen, H.J. Lezec, H.F. Ghaemi, et al., Nature 391 (1998) 667 London.
[2] J.A. Sanchez-Gil, A.A. Maradudin, Phys. Rev. B 60 (1999) 8359.
[3] I.I. Smolyaninov, W. Atia, C.C. Davis, Phys. Rev. B 59 (1999) 2454.
[4] E. Ozbay, Science 311 (2006) 189.
[5] D.B. Shao, S.C. Chen, Appl. Phys. Lett. 86 (2005) 253107.
[6] D.E. Grup, H.J. Lezec, T.W. Ebbesen, et al., Appl. Phys. Lett. 77 (2000) 1569.
[7] A. Degiron, H.J. Lezec, W. Barnes, et al., Appl. Phys. Lett. 81 (2002) 4327.
[8] Y.J. Bao, B. Zhang, J.W. Si, et al., Appl. Phys. Lett. 90 (2007) 251914.
[9] K.L. van der Molen, K.J. Klein Koerkamp, S. Enoch, et al., Phys. Rev. B 72 (2005) 045421.
[10] W.J. Fan, S. Zhang, B. Minhas, et al., Phys. Rev. Lett. 94 (2005) 033903.
[11] J.A. Porto, F.J. Garcia-Vidal, J.B. Pendry, Phys. Rev. Lett. 83 (1999) 02845.
[12] M.M.J. Treacy, Phys. Rev. B 66 (2002) 195105.
[13] R.L. Zhou, X.S. Chen, S.W. Wang, W. Lu, Y. Zeng, H.B. Chen, H.J. Li, H. Xia, L.L. Wang, Solid State Commun. 145 (2008) 23.
[14] Y. Wang, Appl. Phys. Lett. 82 (2003) 4385.
[15] R. Ortuño, C. García-Meca, F.J. Rodríguez-Fortuño, et al., Phys. Rev. B 79 (2009) 075425.
[16] H.J. Li, S.X. Xie, R.L. Zhou, et al., J. Phys.:Condens. Matter 20 (2008) 15223.
[17] H.B. Chan, Z. Marcet, K. Woo, et al., Opt. Lett. 31 (2006) 516.
[18] C. Cheng, J. Chen, D.J. Shi, et al., Phys. Rev. B 78 (2008) 075406.
[19] K.S. Yee, IEEE Trans. Antennas Propag. 14 (1996) 302.
[20] M.A. Ordal, L.L. Long, R.J. Bell, et al., Appl. Opt. 22 (1983) 1099.
[21] P. Drude, Ann. Phys. 306 (1900) 566.
[22] A. Taflove, Computational Electrodynamics: the Finite Difference Time Domain Method, 2nd ed., 2000 Norwood: Artech House.
[23] H.F. Ghaemi, T. Thio, D.E. Grupp, et al., Phys. Rev. B 58 (1998) 6779.
[24] K.J. Klein Koerkamp, S. Enoch, F.B. Segerink, et al., Phys. Lett. 92 (2004) 183901.
[25] Z.C. Ruan, M. Qiu, Phys. Rev. Lett. 96 (2006) 233901.
[26] J.P. Berenger, J. Comput. Phys. 114 (1994) 185.
[27] J.R. Suckling, A.P. Hibbins, M.J. Lockyear, T.W. Preist, J.R. Sambles, C.R. Lawrence, Phys. Rev. Lett. 92 (2004) 147401.
[28] B. Hou, Z.H. Hang, W.J. Wen, et al., Appl. Phys. Lett. 89 (2006) 131917.
[29] B. Hou, J. Mei, M.Z. Ke, et al., Phys. Rev. B 76 (2007) 054303.